

# Superplasticizers and Other Chemical Admixtures in Concrete

Proceedings  
Fifth CANMET/ACI  
International Conference  
Rome, Italy, 1997

*Editor*  
V. M. Malhotra



## High Alumina Cement-Silica Fume Mixtures in the Presence of Superplasticizers

by S. Monosi, R. Troli and M. Collepardi

**Synopsis:** In the presence of silica fume (SF), the hydration of high alumina cement (HAC) produces hexagonal hydrates ( $\text{CaH}_{10}$  and  $\text{C}_2\text{AH}_6$ ) which do not convert into the cubic hydrate ( $\text{C}_3\text{AH}_6$ ) and therefore the related strength loss does not occur: this is due to the formation of  $\text{C}_2\text{ASH}_8$  which blocks the conversion process.

However, due to the presence of SF, the required mixing water significantly increases. Therefore, an effective water reducing admixture is needed to compensate for the presence of SF and to allow the mixture to attain the same strength level of pure HAC at early and later ages.

Two alternative admixtures - sodium triphosphate (TPP) and/or acrylic polymer (AP), instead of other traditional superplasticizers - were studied as water reducers for the blended HAC-SF binder. Both were very effective in reducing the amount of mixing water. However, in the presence of TPP there was a quick fluidity loss after about 45 min. This was a sort of flash set of the binder followed by a sudden heat development. Due to the restrained thermal expansion of the hotter nucleus with respect to the colder surface areas, microcracks formed. Upon contact with liquid water microcracks changed to macrocracks. This severe distress caused a strength failure of the specimens. This change was produced by the pressure exerted by crystal growth of hexagonal hydrates in the water-filled microcracks.

By reducing the fluidity loss - for instance by using AP instead of TPP - the heat development became more gradual and therefore microcracks as well as macrocracks disappeared. Consequently any strength loss was removed in the blended HAC-SF binder.

**Keywords:** High-alumina cements; microcracking; silica fume; superplasticizers

Saveria Monosi is assistant professor of Materials Technology in the University of Ancona. She is author or co-author of numerous papers in the area of concrete durability and chemical admixtures.

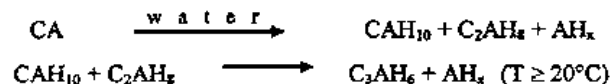
Roberto Troli is a research civil engineer and director of the Enco laboratory. He is author of several papers in the field of concrete technology and in particular of chemical and mineral admixtures.

Mario Collepardi is Professor of Materials Technology and Applied Chemistry in the Ancona University, Italy. He is author or co-author of numerous papers on concrete technology and cement chemistry. He is also the recipient of awards for his contributions to the fundamental knowledge of superplasticizers and their use in concrete.

## INTRODUCTION

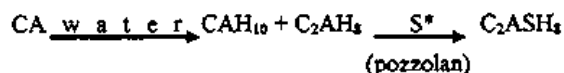
High alumina cement (HAC), based on calcium aluminate (CA), is characterized by high early strength, particularly in cold weather. When, for instance, a compressive strength as high as 20-40 MPa is needed at 6 hours at a temperature as low as 0-5°C, HAC is the unique binder which is capable to meet this requirement. The quick strength increase at very early ages is based on the hydration of CA and the formation of hexagonal hydrates  $CAH_{10}$  and  $C_2AH_6$ .

Unfortunately, at longer ages the strength of HAC may be significantly reduced with time under hot and humid conditions (Fig. 1). Therefore HAC concrete elements are considered to be un-reliable from a structural point of view. The strength reduction at later ages is associated with the conversion of the hexagonal hydrates ( $CAH_{10}$  and  $C_2AH_6$ ) into the cubic hydrate ( $C_3AH_6$ ) which is considered to be the stable phase at higher than ambient temperatures ( $T \geq 20^\circ C$ ):



The strength reduction at later ages (1) is related to the porosity increase of the cement matrix caused by the higher specific gravity of  $C_3AH_6$  with respect to that of  $CAH_{10}$  and  $C_2AH_6$  (2).

In order to hinder the conversion of the hexagonal hydrates into the cubic one, and then to reduce the strength loss at longer ages, Majumdar et al. (3, 4) proposed replacing part of HAC by ground granulated furnace slag, fly ash or silica fume. In the presence of reactive silica ( $S^*$ ) of these pozzolanic materials, hydrated gehlenite ( $C_2ASH_4$ ) is formed at later ages and the conversion into the cubic hydrate is hindered:



The capability of forming  $C_2ASH_4$  either is poor when fly ash is used or requires relatively high percentages of ground slag substituting for HAC (5). In the presence of slag, with typical addition of 40-60%, the blended aluminous cement performs very well in terms of durability or mechanical stability at longer ages (6, 7). Nevertheless, this blended aluminous cement loses the unique early strength performance of the pure HAC, just because of the large replacement of HAC by slag (8).

On the other hand, silica fume (SF) appears to be able to form  $C_2ASH_4$  by replacing smaller percentages (10-20%) of HAC (5). Therefore, this blended aluminous cement is potentially able to attain to approximately the same strength as that of pure HAC. However, because of the high specific surface area of silica fume, the amount of mixing water is increased and again the blended aluminous cement loses the peculiar early strength characteristics of the pure HAC.

## SCOPE OF INVESTIGATION

The present investigation addresses the influence of water reducing admixtures on the HAC-SF system in order to compensate for the increase in the mixing water, caused by the presence of SF, and therefore to allow the mixture to attain the high early strength without any subsequent strength loss at later ages related with the conversion at the hexagonal hydrates into the cubic one. Practical implications of this research relate to HAC-based mortars and concretes when high early strength is needed and mechanical stability at longer is also required.

In a previous paper (1) alternative water reducers - sodium triphosphate (TPP) and acrylic polymer (AP) - were investigated for the HAC-SF system, because traditional superplasticizers (naphthalene-, melamine- or lignosulfonate-based) do not work or act as strong retarders for the HAC hydration. The TPP admixture was very effective in reducing the mixing water and SF was able to block the conversion from the hexagonal hydrates into the cubic phase. Nevertheless, a surprising and un-explained strength loss, associated with significant cracking, was recorded when the HAC-SF binder hydrated in the presence of TPP and was specifically cured at 20°C under water.

The main purpose of the present study was: first, to understand the cracking mechanism responsible for the un-expected strength loss of the HAC-SF binder in the presence of TPP; secondly, to eliminate the cracking process, and therefore to take advantage of the HAC-SF binder in attaining to high-early strength level without any subsequent strength loss.

## TEST PROGRAM

Cement mixtures were manufactured to study the influence of TPP and AP admixtures on the properties of the HAC-SF binder in terms of fluidity, compressive strength and crack formation process. Neat cement paste specimens, instead of mortar or concrete specimens, were studied in the present work in order to have a better evaluation - through XRD and SEM - of the parameters responsible for the cracking process in the cement matrix recorded in a previous work (1).

### Materials

High-alumina cement and silica fume with the chemical composition shown in Table 1, were used to produce a blended binder with 80% of HAC and 20% of SF.

Two chemical admixtures were used: *a*) a solid triphosphosphate, which was proposed as deflocculating agent for the HAC-SF binder by Marcargent et al. (9); *b*) a 30% aqueous solution of acrylic polymer which was proposed by Colleparidi et al. (10) as low slump-loss superplasticizer for portland cement mixes.

Table 1 shows the composition of the cement paste mixtures used in the present work: the water to binder ratio (*w/b*) was always 0.30 except for the reference mixture which required a higher *w/b* (0.45) to attain to a plastic consistency measurable through a modified Marsh cone test.

### Methods

After mixing all the ingredients for 5 minutes, a modified Marsh cone test was used to compare the fluidity of the superplasticized cement mixtures and that of the reference mixture characterized by a tixotropic behaviour for the presence of 20% SF without chemical admixture. Even with the higher *w/b*, the reference mixture was so sticky that some vibration was needed to measure the flow time through the Marsh cone test. The time required for 600 cm<sup>3</sup> of cement paste to leave the Marsh cone test, filled with 900 cm<sup>3</sup> of paste and placed on a Vebe vibrating table (Fig. 2), was measured: the lower was the flow time, the more flowable was the cement paste.

Cement paste specimens (40x40x160mm) were cured at 20°C, demoulded at 6 hr and then immersed under water at 20°C: this wet curing condition was adopted since it was found to favor the crack formation process in the specimens with SF and TPP (1). An alternative humid curing condition - without liquid water - was also adopted by keeping the specimens at 20°C with 95% R.H. after demoulding at 6 hours.

Compressive strength was measured by crushing the extreme 40 mm square areas of the prism specimens (40x40x160 mm): the mean value of the two individual measurements was determined for each specimen as a function of the curing time from 6 hours to 6 months.

Optical microscope and visual observations were used to study the evolution of micro- and macro-cracking respectively.

The XRD technique was adopted to study the change in mineralogical composition of the hydrated cement paste, whereas SEM, with the microprobe chemical analysis (EDAX) was used to observe the inside fractured surface close to the cracked area.

## TEST RESULTS

### Fluidity

Figure 3 shows the fluidity loss curves of the cement mixtures. Both the TPP and AP chemical admixtures reduced significantly the viscosity of the reference HAC-SF binder: from 35 to 5 sec in terms of flow time after 5 min of mixing. This corresponded to a change from a sticky reference mixture to very fluid cement mixes with TPP or AP. Negligible changes in the fluidity with time were recorded for all the mixtures, up to about 40-50 min after mixing. However, at this time, in the presence of TPP, there was a quick and sudden fluidity loss - corresponding to a sort of delayed flash set - and no further fluidity measurement was allowed (flow time = ∞). In the presence of AP, the fluidity decreased much more gradually.

### Compressive Strength and XRD Analysis

Figure 4 shows the compressive strength results of the specimens cured under water. The compressive strength of the reference mixture (HAC-SF system) was lower with respect to a pure HAC paste (1) because of the higher water to cement ratio caused by the presence of silica fume. Due to reduction in the *w/b* (from 0.45 to 0.30), the early compressive strength of superplasticized HAC-SF mixtures were significantly higher than that of the reference mixture (Fig. 4) and very close to the early strength of the pure HAC at 20°C (Fig. 1). At longer ages, there was no strength loss in HAC-SF mixes, except for the specimens with TPP cured under water (Fig. 4).

The XRD analysis indicated that no cubic hydrate formed yet at 180 days of wet curing: Fig. 5 shows comparative XRD patterns of pure HAC paste (where the conversion of CAH<sub>10</sub> and C<sub>2</sub>AH<sub>8</sub> into C<sub>3</sub>AH<sub>6</sub> really occurred between 28 and 180 days) and HAC-SF binder with 0.6% TPP where the formation of

$C_2ASH_6$  blocked completely the conversion of  $CAH_{10}$  and  $C_2AH_6$  into  $C_3AH_6$  at later ages. In the HAC-SF binder with the AP-admixture neither the conversion from hexagonal hydrates into the cubic  $C_3AH_6$  was recorded, nor significant differences in strength were found between under water and 95% RH curing conditions.

Therefore the un-expected strength loss of the HAC-SF-TPP system, which occurred between 7 and 28 days when the specimens were cured under water but not at 95% R.H. (Fig. 6), should be related with something other than the conversion from hexagonal hydrates into the cubic one. Moreover, according to the results of the next section, the strength failure of the HAC-SF binder with TPP was accompanied by a severe cracking process.

#### Cracking and Optical Microscope Observations

Figure 7 shows the typical appearance of cracked specimens of HAC-SF with 0.6% TPP, cured under water for at least a couple of weeks. Before this time, cracks are not visible to the naked eye, but by optical microscope microcracks (about 0.01-0.10 mm wide) could be observed. Figure 8 schematically summarises the cracking evolution map in the HAC-SF-TPP specimens demoulded at 6 hours and then immediately immersed under water. After demoulding and during the initial days (Fig. 8a) only short transverse microcracks (few millimetre long) appeared on the four long edges (160 mm) of the specimen. Between 5 and 10 days (Fig. 8b) the transverse microcracks grew in length (up to 20 mm) and width (up to 0.1 mm), but in general they were not yet visible by the naked eye. Moreover new linear microcracks (160 mm long) formed in this period of time on each face of the specimens. Finally, between 10 and 20 days (Fig. 8c); all the previously formed microcracks transformed into visible macrocracks (up to 1 mm wide) and a quick loss in compressive strength was recorded (Fig. 4).

On the other hand, in the corresponding HAC-SF-TPP specimens cured at 95 R.H. only few short microcracks on the edges were observed. However, they never changed into macrocracks. The XRD pattern did not evidence any difference, between under water specimens and those cured at 95% R.H., which could explain the different crack evolution process. Therefore, it was excluded that any specific chemical change, related with TPP, could be responsible for the strength loss (Fig. 4) and the concurrent macrocracking process (Fig. 8c), although these phenomena occurred in the presence of one chemical admixture (TPP) but not of the other (AP). On the other hand, cracking promoted by drying-shrinkage was also excluded since macrocracks formed only on the surface of the HAC-SF-TPP specimens cured under water, but not in those exposed to the 95% R.H. ambient. Incidentally, it was found that by prolonging the demoulding time from 6 hours to several days, microcracks as those of Fig. 8a again formed immediately, but they did not transform into macrocracks when immersed in liquid water.

#### SEM Observations

In order to examine the reasons why microcracks changed into macrocracks (Fig. 8) and caused strength loss in the HAC-SF-TPP system cured under water (Fig. 4), some specimens were mechanically fractured along the cracked cross section area. Figure 9 shows the picture of one of these typical specimens fractured after 20 days of water curing at 20°C. Four zones can be typically distinguished on each cross section fractured area. The black coloured a zone corresponds to the sound un-cracked nucleus (20-25 mm wide) of the specimen with a very dense microstructure substantially based on fibrous  $C_2ASH_6$  and traces of microcrystallized  $CAH_{10}$  hydrates (Fig. 10a). On the b zone (about 10 mm wide), which is a little less dark than the a zone, some ill-crystallized hexagonal hydrates ( $CAH_{10}$ ) formed on the surface of a very dense substrate (Fig. 10b). The surface of the c zone (about 5 mm wide) looks much brighter than the others and contains numerous large and well crystallized hexagonal plates placed on a very dense substrate (Fig. 10c): the EDAX analysis of the fractured surface evidenced the presence of pure crystallized  $C_2AH_6$ ; on the other hand, the EDAX analysis evidenced primarily Si, Al and Ca elements (or Al with Ca element in smaller areas) in the dense substrate in agreement with the presence of  $C_2ASH_6$  accompanied by smaller amounts of  $CAH_{10}$  and  $C_2AH_6$ . The d zone (1-2 mm wide) is the outer area of the fractured cross section surface. It looks like the inside b zone for the colour as well as for the microstructure.

Figure 11 shows the XRD patterns of samples taken from the above zone a, b, c and d which confirm the above assumptions based on SEM observations supported by EDAX analysis.

#### Interpretation of the Results

All the above available results would indicate the delayed flash set of the HAC-SF-TPP binder - suddenly after the early period of high fluidity (Fig. 3) - as responsible for the strength loss (Fig. 4) through the initial cracking formation process (Fig. 8a).

In the absence of liquid water, microcracks do not grow in width and length and therefore there is no subsequent strength loss (Fig. 6). On the other hand, in the presence of liquid water,  $Ca^{+2}$ ,  $Al^{+3}$ , and  $OH$  ions from the inside microcracked surfaces may dissolve into the water-filled space of the voids and produce crystallized secondary hexagonal hydrates between the inside surfaces of the original substrate. The growth of the hexagonal crystals would be responsible for the opening of the initial microcracks (Fig. 8a) and their change into the final macrocracks (Fig. 8c). Therefore a crack growth mechanism - like that for the delayed ettringite formation (DEF) in microcracked portland cement concrete structures (11) - seems to be responsible for the distress of the

HAC-SF-TPP specimens. Moreover by prolonging the demoulding time from 6 hours to several days, microcracks as those of Fig. 8a again formed immediately, but were no more able to change into macrocracks (12); the delayed immersion in liquid water of the HAC-SF-TPP specimens reduced the capability of  $\text{Ca}^{+2}$ ,  $\text{Al}^{+3}$ , and  $\text{OH}^-$  ions to dissolve into the water-filled microcracks, increased the tensile strength of the specimen and then decreased the wedge pushing effect of the pressure crystal growth.

Depending on the local ionic concentration of  $\text{Ca}^{+2}$ ,  $\text{Al}^{+3}$ , and  $\text{OH}^-$ , as well as on the available space width of the voids,  $\text{C}_2\text{AH}_8$  or  $\text{CAH}_{10}$  can grow in different crystal sizes: cracks in the outside area of the specimen (d zone on Fig. 9) are wider than the other inside deep cracks; however, the local ionic concentration in the d zone would be lower with respect to the deeper c zone because of the diluting effect caused by the outside liquid water in contact with the specimens. This combined action - ionic concentration and crack width - can explain why well crystallized  $\text{C}_2\text{AH}_{10}$  form preferentially in the c zone, whereas ill-crystallized  $\text{CAH}_{10}$  may be found in b and d zones.

There is a last key-point to be discussed: why the delayed flash set of the HAC-SF binder with 0.6% TPP (Fig. 3) is related with the edge microcracks which form transversally with respect to the length of the specimen (Fig. 8a). Really, flash set is not responsible by itself for the initial microcracking of the specimens. It is rather a concurrent phenomenon or a fore-runner of quick heat development, producing a sudden temperature gradient between the hotter nucleus and the colder outside surface of the specimen. Therefore, compressive and tensile stresses are produced between the nucleus and the surface, because of the restrained thermal expansion of the former with respect to the latter.

This proposed mechanism - based on the sudden thermal gradient between nucleus and outside surface area of the cement paste specimen - is confirmed by the following facts. The initial microcracks started by forming on the edges (Fig. 8a) - the coldest area of the specimen because of better heat dissipation - rather than on the middle of the specimen's six faces. Moreover, microcracking decreased in HAC-SF-TPP mortar or concrete specimens due to the lower amount of cement content and the related reduction in heat development, provided that small specimens were manufactured (12). Nevertheless microcracking could again occur when massive concrete structures (150 mm thick) should be produced by using the HAC-SF binder in the presence of TPP (13). Finally, no microcrack at all was recorded when the slope of the fluidity curves (Fig. 3) were not as steep as that in the presence of TPP: the more gradual fluidity loss of the reference HAC-SF binder, or that of the HAC-SF mixture with the AP- admixture, is indicative of a slower heat development rate and therefore of a lower temperature gradient between the nucleus and the outside surface of the specimen.

## CONCLUSIONS

Silica fume acts as a  $\text{SiO}_2$  source which is capable of forming  $\text{C}_2\text{ASH}_8$  as the main component of hydrated HAC. This hinders or blocks the conversion of hexagonal hydrates ( $\text{CAH}_{10}$  and  $\text{C}_2\text{ASH}_8$ ) into the cubic phase ( $\text{C}_3\text{AH}_6$ ), and, therefore, reduces or removes the related strength loss at longer ages generally recorded in HAC concrete structures.

Water reducers are needed to compensate for the higher amount of mixing water required by the presence of silica fume. Sodium TPP and AP are more effective as water-reducing admixtures for the blended HAC-SF binder rather than the traditional melamine-, naphthalene-, or lignosulphonate- based admixtures.

However, TPP causes microcracks on the outside surface area of the specimens which are related to a delayed fast set producing a sudden heat development and restrained thermal expansion of the nucleus with respect to the colder outside surface areas.

Microcracks in the HAC-SF-TPP system can change into macrocracks and cause a dramatic strength failure when the microcracked specimens are exposed to liquid water at an early age.

The mechanism responsible for the change of microcracks into macrocracks is based on the pressure crystal growth of hexagonal hydrates (specially  $\text{C}_2\text{AH}_8$ ) in the water-filled space of the microcracks.

This distress does not occur when the blended HAC-SF binder is treated with AP: due to a more gradual fluidity loss and a reduced thermal gradient between the nucleus and the outside surface area, microcracks do not form and the strength of the blended HAC-SF binder does not decrease at later ages even when exposed to liquid water.

## ACKNOWLEDGEMENT

The work in preparing the text and the Figures by Romina Boaretto and Alessandra Gallerti is acknowledged.

## REFERENCES

1. Monosi, S., Troli, R., Coppola, L. and Collepardi, M. "Water Reducers for the High Alumina-Silica Fume System", *Materials and Structures*, 29, 1996, pp. 519-525.

2. Midgley, H.G. and Midgley, A. "The Conversion of High Alumina Cement", Magazine of Concrete Research, 27, 1975, pp. 59-77.
3. Majumdar, A.J., Singh, B. and Edmonds, R.N. "Hydration of Mixtures of Cement Fondu Aluminous Cement and Granulated Blast Furnace Slag", Cement and Concrete Research, 20, 1990, pp. 197-208.
4. Majumdar, A.J. and Singh, B. "Properties of Some Blended High-Alumina Cements", Cement and Concrete Research, 22, 1992, pp. 1101-1114.
5. Collepardi, M., Monosi, S. and Piccioli, P. "The Influence of Pozzolanic Materials on the Mechanism Stability of Aluminous Cement", Cement and Concrete Research, 25, 1995, pp. 961-968.
6. Osborne, G.J. "BRECEM: A Rapid Hardening Cement Based on High Alumina Cement", Proceedings of Institution of Civil Engineers, 104, 1994, pp. 93-100.
7. Osborne, G.J. "Performance of High Alumina Cement/ Blastfurnace Concretes in Aggressive Environemnts", Proceedings of CONSEC '95, International Conference on Concrete Under Severe Conditions - Environment and Loading, Tapan, E. and F.N. Spon, Vol. 2, Part 22, No. 128, June 1995, pp. 1302-1314. Editors: K. Sakai, N. Branthia and O.E. Gierv.
8. Collepardi, M., Monosi, S. and Mondini, A. "The Influence of Granulated Blast Furnace Slag on the Mechanical Stability of High-Alumina Cement" (in Italian), L'Edilizia, 3, 1994, pp. 47-51.
9. Marcargent, S., Testud, M., Bayoux, J.P. and Mathieu, A. "Hydration and Strength of Blends CAC- Silica Fume and Stability of Hydrates", Proceedings of the IX International Congress on the Chemistry of Cement, New Delhi, Vol. 4, 1992, pp. 651-657.
10. Collepardi, M., Coppola, L., Cerulli, T., Ferrari, G., Pistolesi, C., Zaffaroni, P. and Quek, F. "Zero Slump-Loss of Superplasticized Concrete", Proceedings of the Congress "Our World in Concrete Structures", Singapore, 1993, pp. 73-80.
11. Mielenz, R.C., Marusin, S.L., Hime, W.G. and Jugovic, Z.T. "Investigation of Prestressed Concrete Railway Tie Distress", Concrete International, 12, 1995, pp. 62-68.
12. Troli, R. "Utilization of High Alumina Cement in Tunnels Construction by Using the Pre-Mill Technique" (in Italian), Graduation Thesis in Civil Engineering, Department of Science of Materials and Earth, University of Ancona, Italy, 1994.
13. Coppola, L. (private communication).

TABLE 1 - COMPOSITION OF PASTE MIXTURES

Ingredient	Composition (mass parts) for:		
	Plain Mix	TPP Mix	AP Mix
HAC	80	80	80
SF	20	20	20
TPP	-	0.6	-
AP	-	-	0.9
Water	45	30	30
water/binder	0.45	0.30	0.30

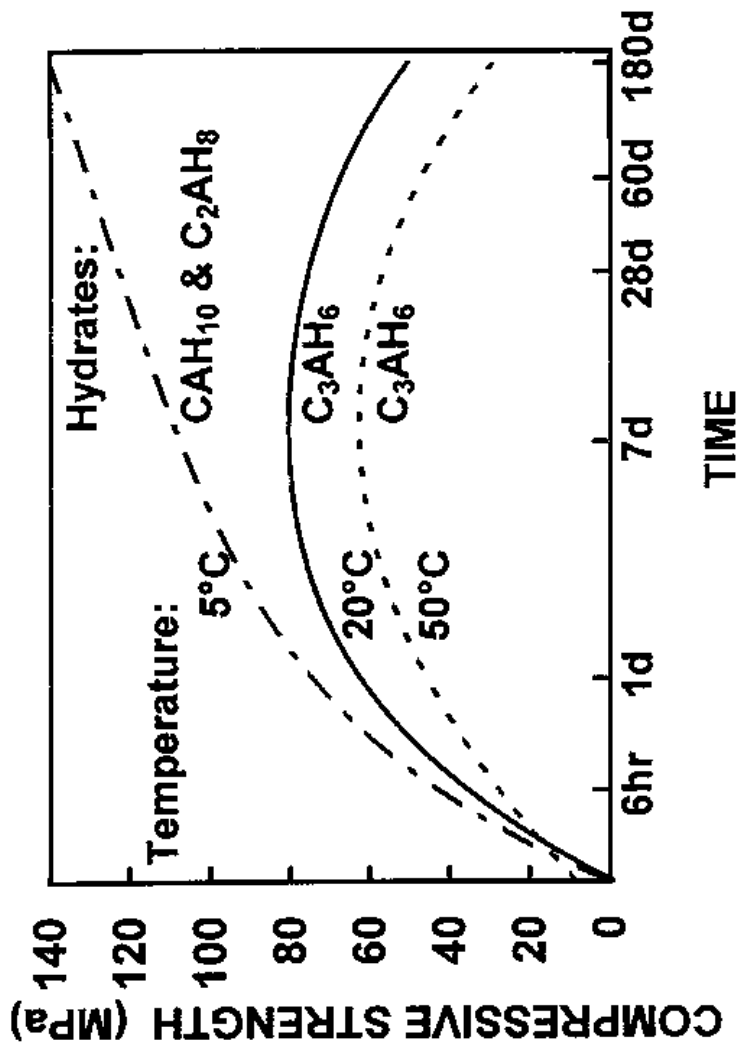


Fig. 1—Schematic trend of compressive strength versus time of high-alumina cement paste with w/c of 0.30, cured under water (1)

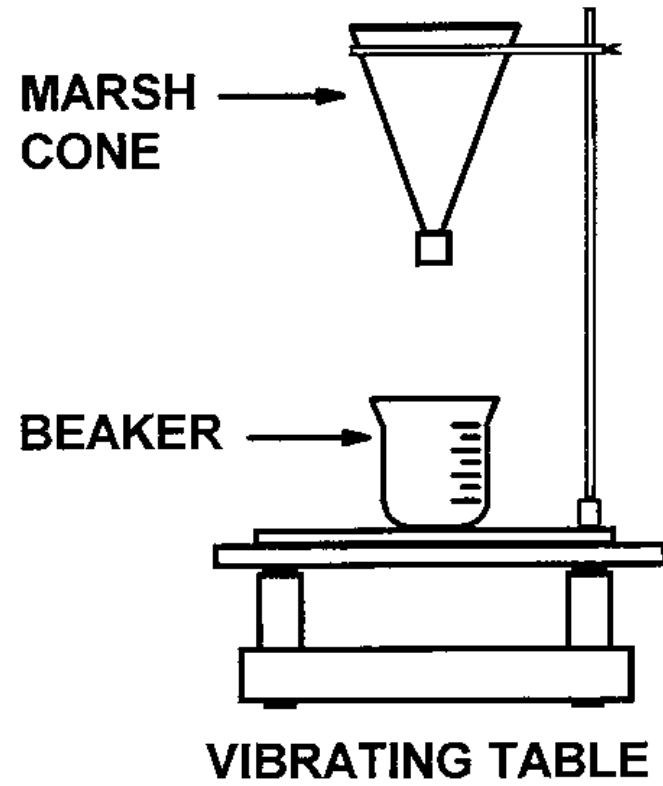


Fig. 2—Modified Marsh cone test to measure the fluidity of the cement paste

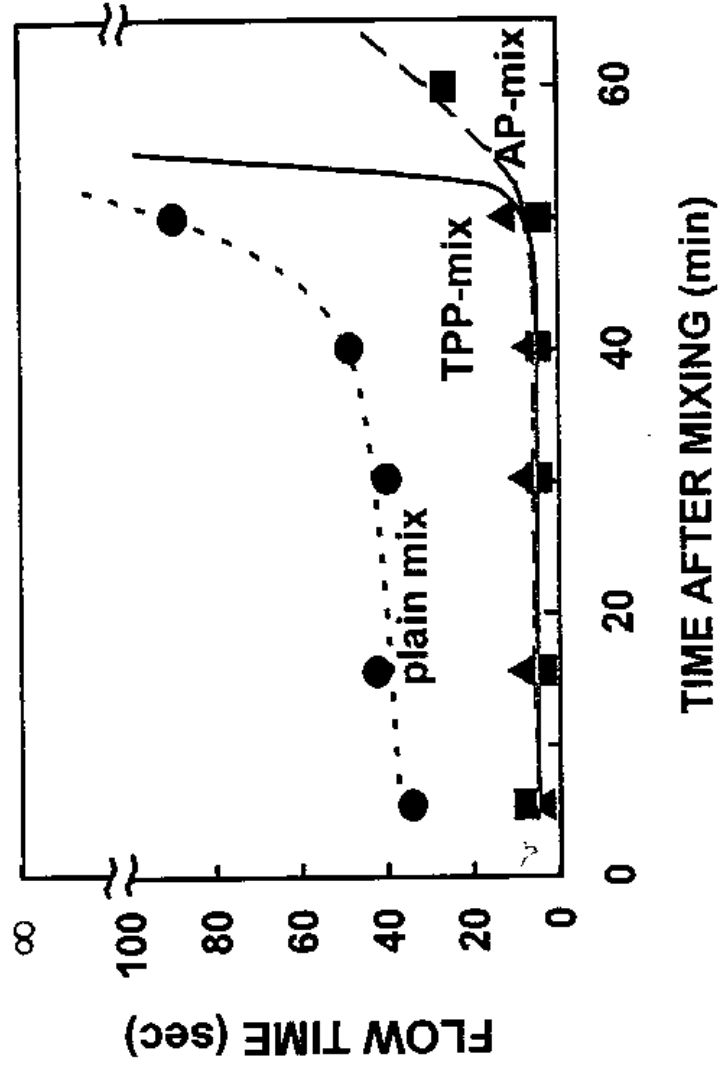


Fig. 3—Fluidity loss curves for the plain HAC-silica fume mix and mixes with TPP of AP

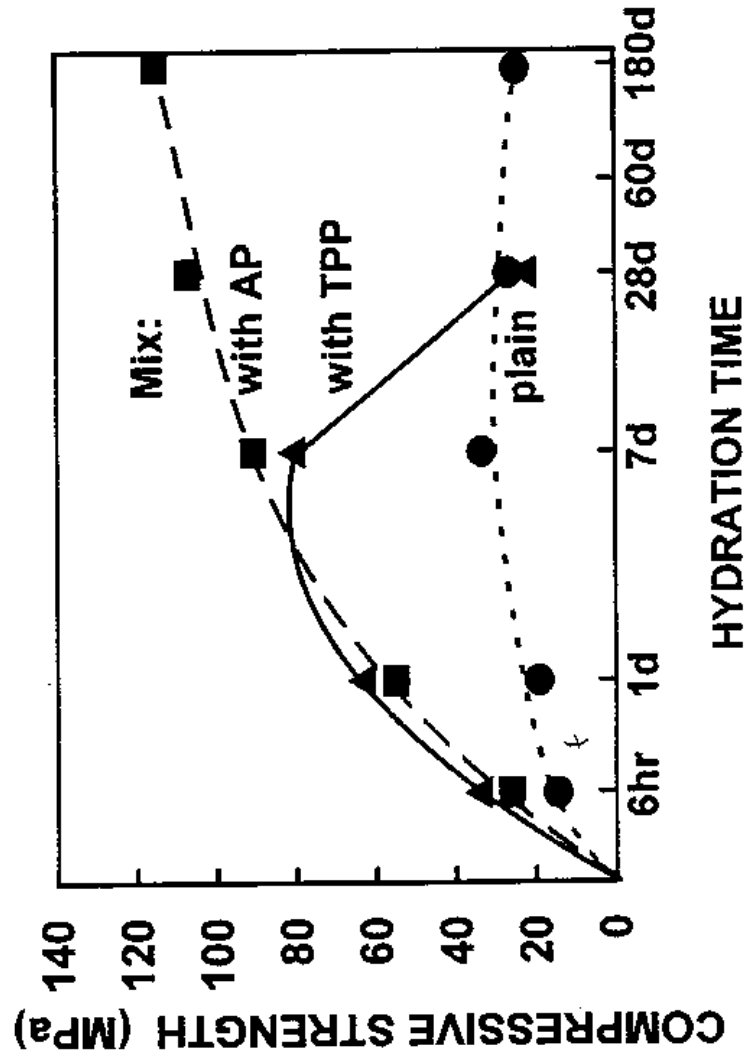


Fig. 4—Influence of AP and TPP admixtures on the compressive strength of the HAC-SF specimens cured at 20°C under water

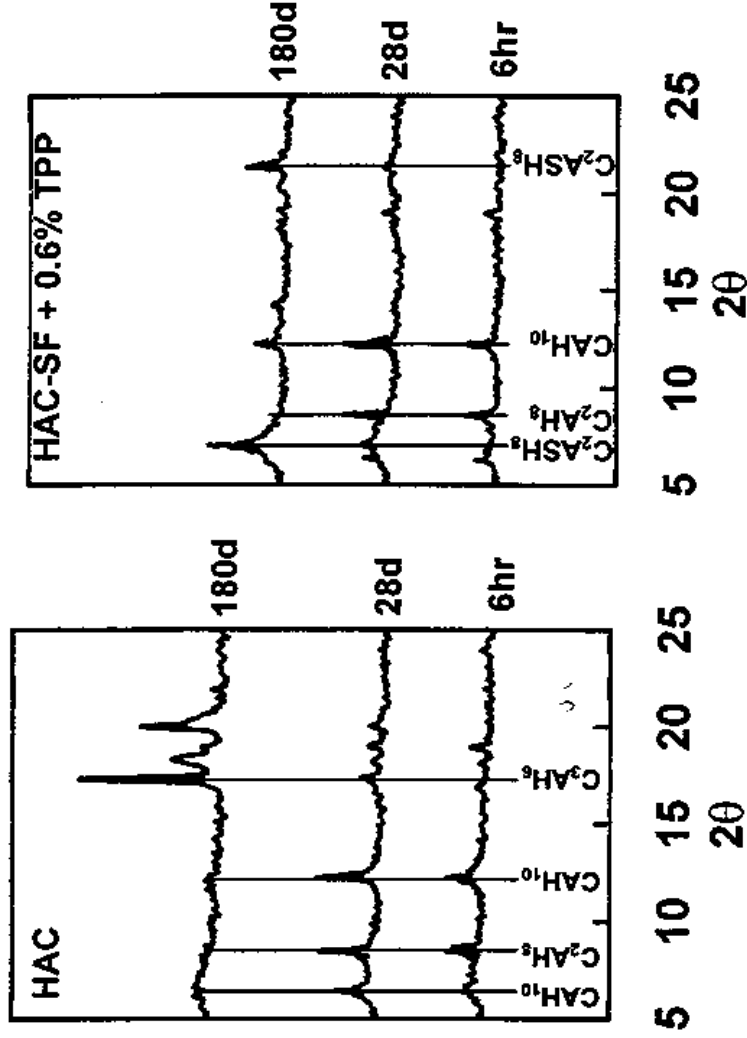


Fig. 5—XRD of pure HAC and HAC-SF binder with 0.6% TPP

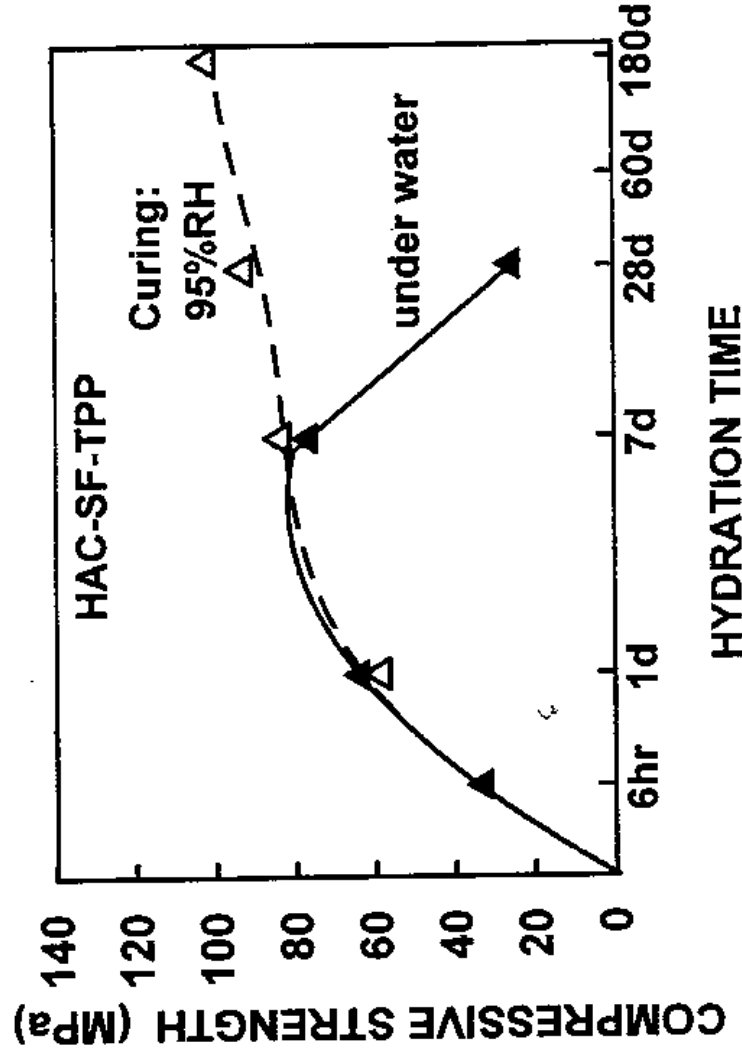


Fig. 6—Influence of the curing on the compressive strength of the HAC-SF system with TPP



Fig. 7—Picture of a macrocracked specimen (HCA-SF-TPP) cured 20 days under water at 20°C

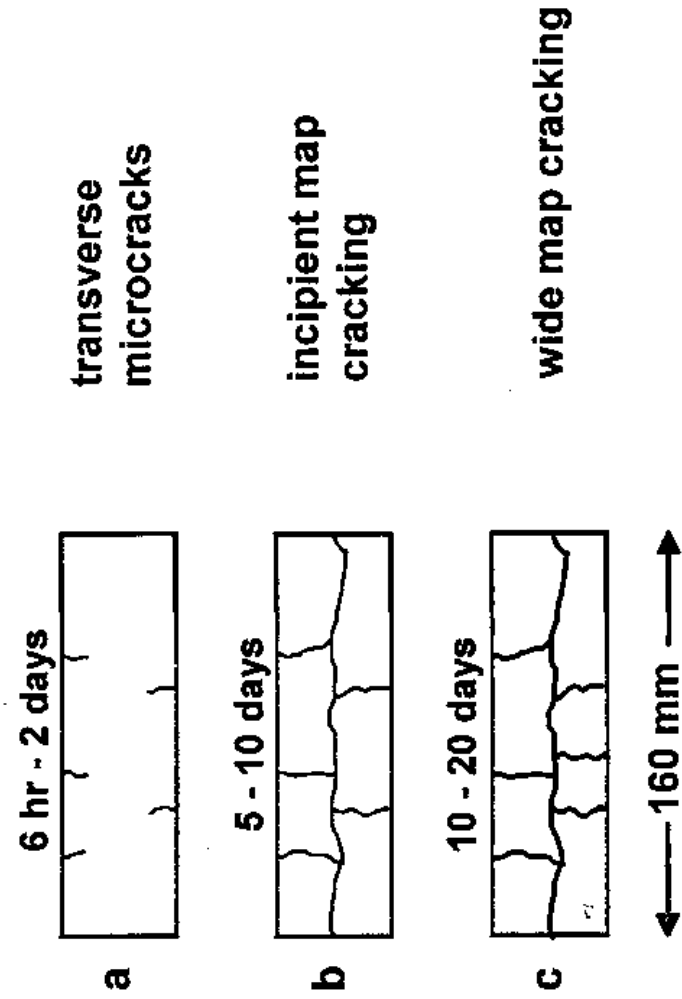


Fig. 8—Crack evolution process of HAC-SF-TPP specimens cured at 20°C under water

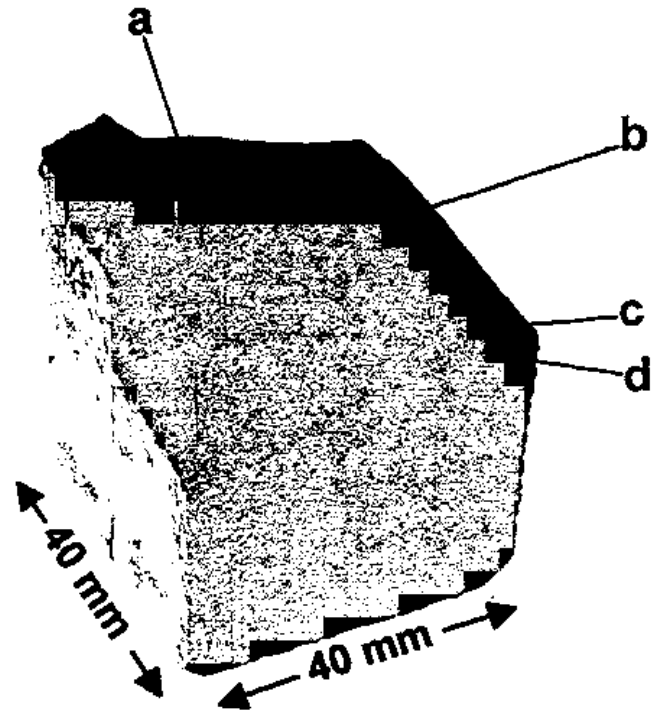
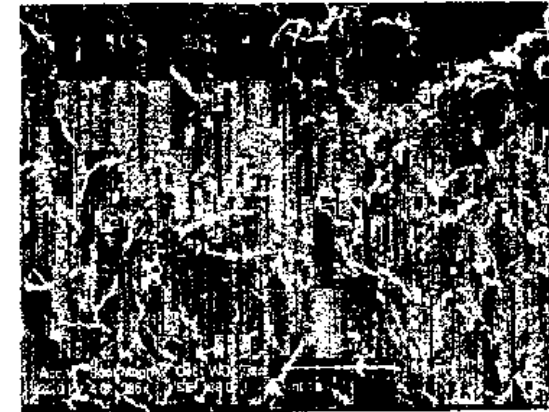


Fig. 9—Transversal inside surface area of an HAC-SF-TPP specimen cured under water 20 days, and then mechanically fractured. The black zone (a) corresponds to the sound nucleus of the specimen. The other zones (b, c and d) correspond to macro-cracked areas



a



c



b&amp;d

Fig. 10—Typical SEM morphologies of zones a, b, c and d of the fractured cross section (see figure 9)

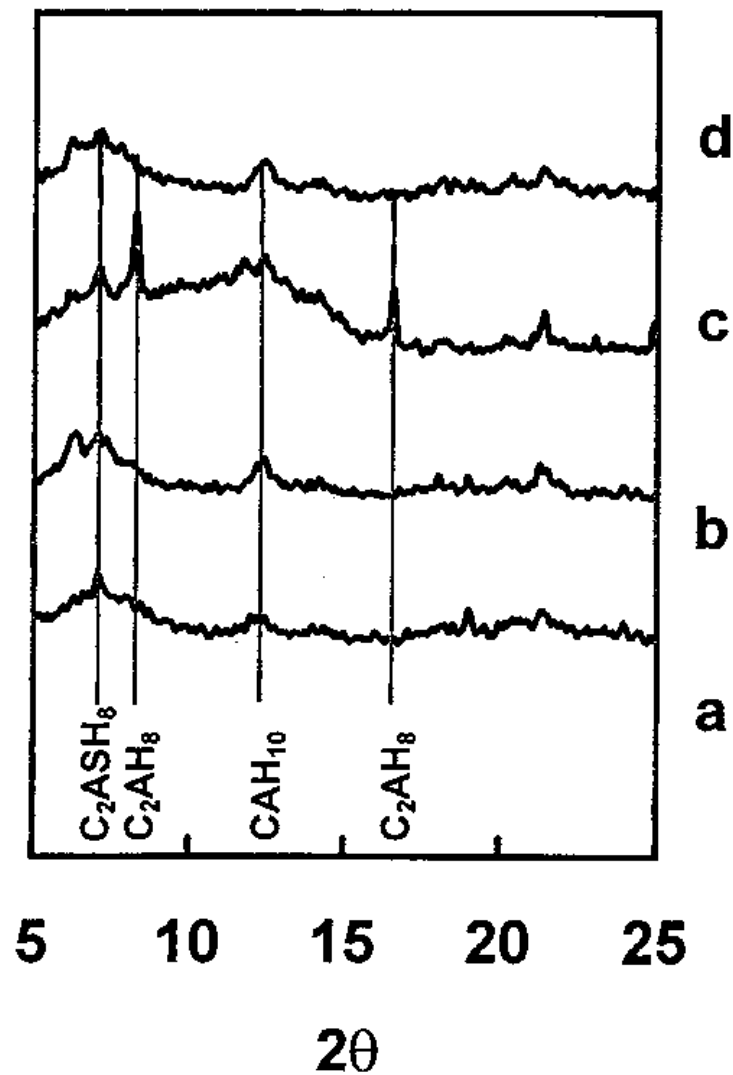


Fig. 11—XRD of samples taken from zone a,b,c and d of the fractured specimen in figure 9

SP 173-32

## Effect of Types of Superplasticizers and Mixing Methods on the Properties of Cementitious Systems

by E. Tazwa, B. Mtasiwa and M. Takahasi

**Synopsis:** This paper reports the properties of cement paste, mortar and fresh and hardened concrete using superplasticizers with electric repulsion, steric barrier and those possessing both dispersing mechanisms and their interaction with cementitious materials having pozzolanic properties and those without pozzolanic properties prepared by different mixing methods. It was found that there is an optimum W/C for the primary water ( $W_1/C$ ) where bleeding is minimum and thus dispersion state is optimum. The fresh properties of concrete prepared by double mixing method are different from those by conventional mixing method (Single mixing). Also, when superplasticizers are added in primary water ( $W_1$ ), fresh properties of concrete are different from those when added in secondary water ( $W_2$ ). The effect of dosing method of superplasticizers and replacement of cement with different cementitious materials, varies greatly with the type of superplasticizers.

**Keywords:** Adsorption; cement pastes; dispersants; mixing; mortars (materials); superplasticizers